EARTHQUAKE ENGINEERING AND STRUCTURAL DYNAMICS
Earthquake Engng Struct. Dyn. 2005; **34**:1353–1374
Published online 1 June 2005 in Wiley InterScience (www.interscience.wiley.com). DOI: 10.1002/eqe.483

Influence of earthquake spatial variability on differential soil displacements and SDF system response

Camillo Nuti[1,‡,¶] and Ivo Vanzi[2,*,†,§]

[1] *Dipartimento di Scienze dell'Ingegneria Civile, University of Rome 3, Rome, Italy*
[2] *Dipartimento di Progettazione, Riabilitazione e Controllo delle Strutture, Pricos, University G. D'Annunzio of Chieti, Pescara, Italy*

SUMMARY

The aim of this study is to develop design criteria, which account for the effects of earthquakes spatial variability. The two simplest forms of this problem are dealt with: differential ground displacements and differential structural displacements, for points and structures separated in space. The structures considered are linear elastic single degree of freedom oscillators. These problems may seem trivial, but some of the codes considered appear improvable on this aspect.

First, the mathematical model is set up using basic random vibration theory and the code provisions critically examined. Then, the sensitivity of the ground and structural differential response is assessed. The differential displacements can be mathematically expressed in a straightforward fashion, both for the ground and the structures. These expressions are simple enough to be used as design rules.

Comparison with the European and Italian Civil Protection codes shows that these can be improved on this aspect; and, for this reason, the Italian draft code for bridges has been mainly drafted following the results of this study. Copyright © 2005 John Wiley & Sons, Ltd.

KEY WORDS: bridge design; earthquake; non-synchronous motion; support design; random field; probability

1. INTRODUCTION AND SCOPE

Simultaneous recordings of earthquakes [1, 2] in different spatial points indicate that the earthquake accelerations differ from one point to the other retaining a degree of similarity that can be quantified in a statistical sense. This experimental observation has led researchers in the last twenty years to develop accurate models to define the behaviour. Departing from the classical work of Luco and Wong [3] in the mid 1980s, different statistical descriptions have been proposed and fitted to the experimental data [1, 2, 4, 5], with varying degree of complexity and accuracy.

*Correspondence to: Ivo Vanzi, Pricos, Viale Pindaro 42, 65127, Pescara, Italy.
† E-mail: i.vanzi@unich.it
‡ E-mail: c.nuti@uniroma3.it
§ Associate Professor.
¶ Full Professor.

Received 22 December 2003
Revised 6 December 2004
Accepted 12 January 2005

In parallel with the study of the ground behaviour, the effects of the earthquake spatial variability on structures have been the object of systematic investigations. Random vibration is a powerful tool for dealing with this problem and it has been extensively used to assess the effects on linear structures. A comprehensive method for response spectrum analyses has been, for instance, presented by Der Kiureghian and Neuenhofer [6, 7].

For non-linear structures, researchers have used either numeric analyses or equivalent linearization procedures [8, 9]. The most important outcome of the studies [10–12] has been unambiguous: apart from a few cases, non-synchronous action decreases the stresses with respect to the case with synchronous actions.

There are, however, situations in which non-synchronism negatively influences structural behaviour, e.g. failure of some bridges during the Loma Prieta earthquake [13]; furthermore, deck unseating is a frequent collapse mode for bridges, clearly governed by differential response, and the design rules provided by the codes appear improvable, at least for the differential displacements of ground and single degree of freedom (sdof) structures. Some codes neglect, implicitly or explicitly, correlations between motions, and inherently fragile failures, like deck unseating, should be dealt with a higher safety margin with respect to the other failure modes.

For the above reasons, this study is focussed on the two simplest effects of non-synchronism: differential displacements of ground and linear elastic sdof structures. The physical model is developed and compared with the European [14], Italian Civil Protection [15] and draft Italian [16] code for bridges. The three codes will be, respectively, indicated with the acronyms EC8, ICPC, DICB from now on. The relative importance of the parameters governing ground and structural behaviour is assessed. Design rules for the codes are proposed and compared with the results of the theoretical model.

The influence of earthquake spatial variability on the differential displacements of ground and sdof structures is a difficult problem to manage. Many parameters are involved, be they soil or structure specific. This study succeeds in identifying the important variables. The model does not account for important effects like soil–structure interaction, particular geological conditions (which may cause the earthquake spatial variability differ from what is assumed), and non-linear behaviour of structures. Therefore, problem-specific analyses will be needed for these cases, e.g. piles foundation in soft soil. This study intends to give systematic organization and solution to the most frequently encountered situations.

In the model development, an interesting problem has been encountered: if the earthquake action is specified in terms of response spectra, which is the case for all the codes, the classical modified Kanai–Tajimi [17, 18] power spectrum representation of the action, needed to quantify the differential displacements, is incompatible with the displacement response spectrum at high periods. The modified Kanai–Tajimi power spectrum has therefore been corrected and the modification factors are one of the results of this paper.

2. MODEL AND DEFINITION OF EARTHQUAKES THAT VARY IN SPACE

2.1. Physical and numeric model of the earthquakes

An earthquake acceleration recording at point P in space can be represented via its Fourier expansion as a sum of sinusoids [5]:

$$A_P(t) = \sum_K [B_{PK} \cos(\omega_K t) + C_{PK} \sin(\omega_K t)] \tag{1}$$

In Equation (1), A is the measured acceleration in point P at time t, K is an index varying from 1 to the number of circular frequencies ω_K considered, B_{PK} and C_{PK} are the amplitudes of the Kth cosine and sine functions. Assume the acceleration $A_P(t)$ is produced by a wave moving with velocity V towards a different point in space, say Q, at distance X_{PQ} from P. At point Q, and at time t, one would have

$$\begin{aligned} A_Q(t) &= \sum_K [B_{QK}\ \cos(\omega_K(t-\tau_{PQ})) + C_{QK}\ \sin(\omega_K(t-\tau_{PQ}))] \\ \tau_{PQ} &= \frac{X_{PQ}}{V} = X_{PQ}\left(\frac{\cos(\psi)}{v_{\text{app}}}\right) \end{aligned} \tag{2}$$

In Equation (2) ψ is the angle between the vector of surface wave propagation and the vector that goes from P to Q, τ_{PQ} is the time delay of the signal and v_{app} is the surface wave velocity. The amplitudes B_{QK} and C_{QK} would be, respectively, equal to B_{PK} and C_{PK} if the medium through which the waves travel did not distort them. In a real medium, B_{PK} is correlated with B_{QK} and C_{PK} is correlated with C_{QK} and the B's and C's are independent. The latter is often referred to with the sentence 'phase angles are random'. The amplitudes B_{PK} and C_{QK} are statistically independent, for any points P and Q, and any circular frequency ω_K, with the only exception of B_{PK} and B_{QK}, i.e. same circular frequency but different points in space. The same holds for C_{PK} and C_{QK}. The amplitudes are assumed normally distributed with zero mean and this assumption is experimentally verified [5]. In order to quantify the acceleration time histories in different points in space, Equations (1) and (2), all that is needed is a definition of the correlation between amplitudes and of their dispersion, as measured by the variance or, equivalently, of the covariance matrix of the amplitudes. Numerical methods for amplitudes sampling, which allow to reconstruct the whole earthquake accelerations random field, can be found in References [5, 19, 20]. The signal components for different circular frequencies, once the amplitudes are sampled, can be computed in an efficient way by doing an inverse Fourier transform, possibly using the fast Fourier algorithm [21].

The covariance matrix Σ of the amplitudes B and C is assembled via independent definition, at each circular frequency ω, of its diagonal terms, the variances in each space point and frequency, and of the correlation coefficients. The diagonal terms Σ_{PP} are quantified via a power spectrum. A traditional choice is the Kanai–Tajimi power spectrum, as modified by Clough and Penzien [21]:

$$\begin{aligned} G_{PP}(\omega) &= G_0\,\frac{\omega_f^4 + 4\beta_f^2\omega_f^4\omega^2}{(\omega_f^2-\omega^2)^2 + 4\beta_f^2\omega_f^4\omega^2}\,\frac{\omega^4}{(\omega_g^2-\omega^2)^2 + 4\beta_g^2\omega_g^4\omega^2} \\ \Sigma_{PP} &= G_{PP}(\omega)\,\mathrm{d}\omega \end{aligned} \tag{3}$$

The Kanai–Tajimi power spectrum is herein adopted with a modification discussed in Section 4. The correlation coefficient between the amplitudes is expressed via the coherency function: the form originally proposed by Uscinski [22] on theoretical grounds and Luco [3] is retained:

$$\rho = \exp\left(-\omega^2 X^2\left(\frac{\alpha}{v}\right)^2\right) \tag{4}$$

The correlation decreases with increasing distance X and circular frequency ω and increases with increasing soil mechanical and geometric properties as measured by v/α. α is the incoherence parameter, v the shear wave velocity. Equation (4) is extensively used [6–8, 23–26], but different functional forms have also been proposed. v may be estimated as $(G_{\text{soil}}/\rho_{\text{soil}})^{0.5}$ with G_{soil} and ρ_{soil}, respectively, the ground shear modulus and density. The incoherence parameter α is the most difficult aspect in the coherency function assessment. Zerva [25] and Luco and Mita [27] report a value in the range of 0.1–0.5. Der Kiureghian and Neuenhofer [7] use for $[X\alpha/v]$ a value within 0–2, which is in line with what is expected in the two previous papers. Numerical comparison of Equation (4) with some of the experimental data for different soil types has also been made within this study. The 0.1–0.5 range is generally confirmed. Some events showed, however, an even smaller lower bound. To name a few, all the events recorded at Parkfield, California, and most events recorded in Taiwan on the SMART array, as reported by Abrahamson *et al.* [1], fall within 0.1–0.5, but event 45 reported by Oliveira [2] in Taiwan has a value for α of about 0.02. The soil in Parkfield is rocky, while the one in Taiwan is alluvium. For the above reason, a range for α as large as 0.02–0.5 is kept in this study.

Equations (2) and (4) can be adapted to the case of soil discontinuities. This aspect is dealt with in a recent paper [28], but some further remarks seem convenient. With reference to Figure 1, one has to determine equivalent v/α and v_{app}. For v_{app}, the equivalent value can be obtained with a weighted average on the distances:

$$v_{\text{app}} = \xi_1 v_{\text{app1}} + \xi_2 v_{\text{app2}}$$
$$\xi_1 + \xi_2 = 1 \tag{5}$$

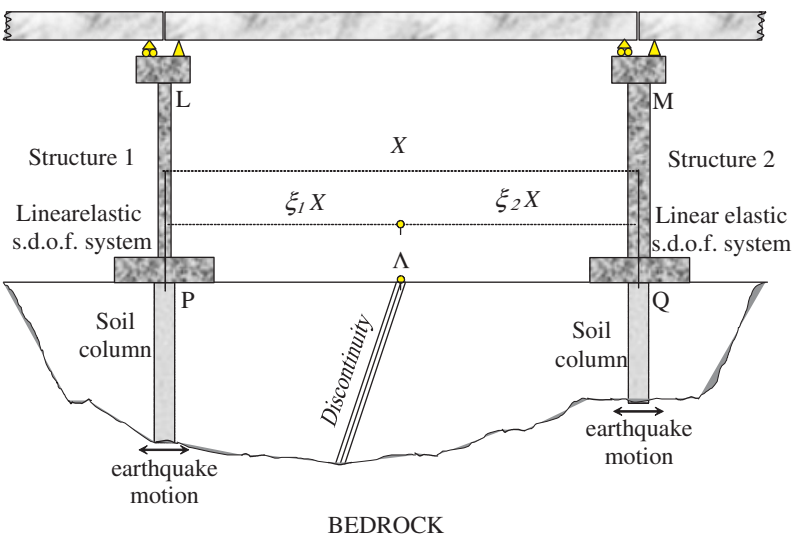

Figure 1. Geometry for soil discontinuity and for the structure.

Derivation of equivalent v/α is instead less straightforward. Equation (4) can be recast in the form

$$\rho_{PQ} = \rho(X_{PQ}) = \left[\exp\left(-\omega_K^2 \left(\frac{\alpha}{v}\right)^2 X_{PQ}^2\right)\right]$$

$$= \left[\exp\left(-\omega_K^2 \left(\frac{\alpha}{v}\right)^2 (\xi_1 X_{PQ} + \xi_2 X_{PQ})\right)\right]^{(\xi_1 X_{PQ} + \xi_2 X_{PQ})} \tag{6}$$

After rearranging terms it can be written as

$$\begin{aligned} \rho_{PQ} &= \rho_{P\Lambda}\rho_{Q\Lambda} \\ \rho_{P\Lambda} &= \rho(\xi_1 X_{PQ})\rho(\sqrt{\xi_1(1-\xi_1)}X_{PQ}) \\ \rho_{Q\Lambda} &= \rho(\xi_2\ X_{PQ})\rho(\sqrt{\xi_2(1-\xi_2)}\ X_{PQ}) \end{aligned} \tag{7}$$

Equation (7), valid for homogeneous soil, provides a convenient way to separate the loss of correlation along the distance X_{PQ}. The $\rho_{P\Lambda}$ can be thought of as the loss of correlation due to the travelling of the waves from P to Λ, $\rho_{Q\Lambda}$ and from Λ to Q. For the case of two soil types, say 1 and 2, the equivalent properties of v/α can be obtained from (7) as

$$\frac{\alpha}{v} = \sqrt{\left(\frac{\alpha_1}{v_1}\sqrt{\xi_1}\right)^2 + \left(\frac{\alpha_2}{v_2}\sqrt{\xi_2}\right)^2} \tag{8}$$

For the case of N soil types it can be shown that

$$\frac{\alpha}{v} = \sqrt{\sum_{h=1}^{N}\left(\frac{\alpha_h}{v_h}\sqrt{\xi_h}\right)^2} \tag{9}$$

while for v_{app} it is straightforward that

$$\begin{aligned} v_{\text{app}} &= \sum_{h=1}^{N} \xi_h v_{\text{app\_}h} \\ \sum_{h=1}^{N} \xi_n &= 1 \end{aligned} \tag{10}$$

2.2. *Soil and structure differential displacements*

In this section the differential response to the spatially varying earthquake defined as in Equations (1) and (2) is computed. The problem geometry is in Figure 1. The figure is made with reference to a typical application problem: a simply supported bridge deck, for which one has to compute the seating length. For generality it is assumed that a soil discontinuity is present between points P and Q. Structures 1 and 2 are different, but both are linear elastic. The goal is to compute the differential response between P and Q, points on the soil, and between L and M, located on top of the sdof oscillators.

Basic random vibration theory [29] will be used for this. The input is the accelerations considered frequency component by frequency component (both sine and cosine terms will be considered). After dropping the subscript k, one component of the acceleration time history in Q is

$$A_Q(t) = B_Q \cos(\omega(t - \tau_{PQ})) + C_Q \sin(\omega(t - \tau_{PQ})) \tag{11}$$

The total displacement in $M, Z_M(t)$ is the sum of the ground displacement $Z_Q(t)$ and of the sdof system displacement with respect to the ground $Z_{MQ}(t)$:

$$\begin{aligned} Z_M(t) &= Z_Q(t) + Z_{MQ}(t) \\ Z_Q(t) &= -\frac{A_Q(t)}{\omega^2} \end{aligned} \tag{12}$$

If structure 2, which has damping equal to β_{MQ} and circular frequency equal to ϖ_{MQ}, is subjected to the acceleration $\exp[\mathrm{j}\omega(t - \tau_{PQ})]$, with j the imaginary unit, its displacement $Z_{MQ}(t)$ relative to the ground is

$$\begin{aligned} Z_{MQ}(t) &= H(\varpi)\, \exp(\mathrm{j}\omega t) \exp(-\mathrm{j}\omega\tau_{PQ}) \\ H(\varpi) &= \frac{-1}{(\varpi^2 - \omega^2) + \mathrm{j}(2\beta\varpi^2\omega)} \end{aligned} \tag{13}$$

After expressing the input in the imaginary field, and after performing some algebra (see Reference [20]), it can be shown that the differential displacements (both absolute and relative) for points L, P, M and Q, are independent of time and are normally distributed:

$$\begin{aligned} Z^*(t, m_1, m_2, n_1, n_2) &= Z^*(m_1, m_2, n_1, n_2) \sim N(\mu = 0, \sigma^2_{Z^*}) \\ \sigma^2_{Z^*} &= \Delta\omega \sum_K G_{Z^*K} \\ G_{Z^*K} &= \sigma^2_{PK} + \sigma^2_{QK} - \sigma_{PQK} \\ \sigma_{PQK} &= 2\sigma_{PK}\sigma_{QK}[\rho_{PQK} \cos(\gamma_{PK} - \gamma_{QK} - \omega_K\tau_{PQ})] \\ \sigma^2_{PK} &= N^2_{PK} G_{PPK} \quad \sigma^2_{QK} = N^2_{QK} G_{QQK} \\ N_P &= -\frac{1}{\omega^2}\sqrt{\frac{m_2 F^2_{P2} + F^2_{P3}}{F^2_{P1} + F^2_{P2}}} \quad N_Q = -\frac{1}{\omega^2}\sqrt{\frac{n_2 F^2_{Q2} + F^2_{Q3}}{F^2_{Q1} + F^2_{Q2}}} \\ \gamma_P &= \arctan\left[\frac{m_2 F_{P2}}{F_{P3}}\right] - \arctan\left[\frac{F_{P2}}{F_{P1}}\right] \quad \gamma_Q = \arctan\left[\frac{n_2 F_{Q2}}{F_{Q3}}\right] - \arctan\left[\frac{F_{Q2}}{F_{Q1}}\right] \\ F_{P1} &= \varpi^2_{LP} - \omega^2 \quad F_{Q1} = \varpi^2_{MQ} - \omega^2 \\ F_{P2} &= 2\beta_{LP}\varpi_{LP}\omega \quad F_{Q2} = 2\beta_{MQ}\varpi_{MQ}\omega \\ F_{P3} &= m_1\varpi^2_{LP} + m_2 F_{P1} \quad F_{Q3} = n_1\varpi^2_{MQ} + n_2 F_{Q1} \end{aligned} \tag{14}$$

Equation (14) gives both the power spectrum and the variance of the differential displacements Z^* for points P, Q, L and M, within a single expression. $m_{1,}, m_2, n_1, n_2$ are equal either to zero or to one. Differential ground displacements, between points P and Q, are obtained with $(m_1 = 0, m_2 = 1, n_1 = 0, n_2 = 1)$, structural displacement with respect to ground, between points L and M and with fixed bases, with $(m_1 = 1, m_2 = 0,\ n_1 = 1, n_2 = 0)$, total displacements, between points L and M and with respect to an inertial reference frame, with, $(m_1 = 1, m_2 = 1, n_1 = 1, n_2 = 1)$, any other mixed quantity can be computed, e.g. total displacement in P with respect to ground displacement in $Q (m_1 = 1, m_2 = 1, n_1 = 1, n_2 = 0)$.

The distribution of maxima can be found with the peak factor formulation [30], by setting

$$Z^*_{s,p} = \sigma_{Z^*} r_{s,p} \tag{15}$$

where $Z^*_{s,p}$ is the displacement value, which is not exceeded with probability p during an earthquake of duration s. Typical values of the peak factor $r_{s,p}$ lie within 1.20–3.5; $r_{s,p}$ is computed as set out in Reference [30], in which proper account is taken for the non-stationarity of the response via the use of the equivalent damping.

3. CODE PROVISIONS FOR DIFFERENTIAL DISPLACEMENTS

Codes allow, together with a refined analysis, a simplified one to compute structural differential displacement considering non-synchronism. In the simplified analysis, non-synchronism is the sum of two separate problems: ground differential displacement only (points P and Q in Figure 1) and structural differential displacements with synchronous soil motion (points L and M). The outcomes from the analyses are summed up disregarding their correlation. This is on the safe side (one is adding the modules of correlated displacements). The procedure is justified in view of the fact that the structural analyses are done for stress calculation and that codes have to service designers and hence be simple.

For a comparison, the following codes are considered:

- The European seismic code Ec8 [14], partially adopted in Italy by the Civil Protection [15]. This code will be referred to with EC8/ICPC, meaning EuroCode 8/Italian Civil Protection Code.
- The draft Italian seismic code for bridges [16]. This code will be referred to with DICB, meaning Draft Italian Code for Bridges. This code, for non-synchronism, has been drafted following mainly the results from the present study.

The codes state the ground differential displacements be computed as

$$\left.\begin{array}{c} u^I_{PQ} = X_{PQ}\,\mathrm{pga}\,\dfrac{T_C}{v_{\mathrm{app}}}\left(\varepsilon\,\dfrac{1}{2\pi}\right) \leqslant u^{\mathrm{I\_MAX}}_{PQ} \\ u^{\mathrm{I\_MAX}}_{PQ} \leqslant 0.025\,\mathrm{pga}\,\sqrt{(\varepsilon_P T_{PC} T_{PD})^2 + (\varepsilon_Q T_{QC} T_{QD})^2} \end{array}\right\} \text{EC8/ICPC}$$

$$\left.\begin{array}{c} u^{\mathrm{II}}_{PQ} = \mathrm{pga}\,[q_1 + q_2 \log(X)^{q_3}] \leqslant u^{\mathrm{II\_MAX}}_{PQ} \\ u^{\mathrm{II\_MAX}}_{PQ} \leqslant 1.25 \times 0.025\,\mathrm{pga}\,\sqrt{(\varepsilon_P T_{PC} T_{PD})^2 + (\varepsilon_Q T_{QC} T_{QD})^2} \end{array}\right\} \text{DICB} \tag{16}$$

with

$$\begin{aligned} X_{PQ} &= \text{distance between points } P \text{ and } Q \\ \varepsilon_P &= \text{soil coefficient in point } P \\ \text{pga} &= \text{peak ground acceleration} \\ T_{PC}, T_{PD} &= \text{periods defining the response spectra in point } P \\ v_{\text{app}} &= \text{surface wave velocity} \\ q_1, q_2, q_3 &= \text{coefficients depending on the soils in } P \text{ and } Q \end{aligned} \tag{17}$$

The numeric values of the quantities in Equation (17) will be defined below. The differential displacements of the two points of the structure, u_{LM}, are computed with a response spectrum analysis, with synchronous motion. This means that for two sdof structures, the complete quadratic combination [31], CQC, rule will be used. The total differential displacements prescribed by the codes are

$$\begin{aligned} \{U^{\text{I}}_{LM} = u^{\text{I}}_{PQ} + u_{LM}\}\text{EC8/ICPC} \\ \{U^{\text{II}}_{LM} = u^{\text{II}}_{PQ} + u_{LM}\}\text{DIC} \end{aligned} \tag{18}$$

The DICB explicitly permits to compute u_{LM} with the square root of sum of squares (SRSS) rule; in case of fragile failures, e.g. deck unseating, the final results, be it the soil or structural differential displacements, are multiplied by 1.25.

The parameters in Equations (16) and (18) are shown in Table I for the EC8/ICPC code and Table II for the DICB. For both codes reference is made to the ultimate limit state.

The codes group the grounds into two homogeneous types. The first group is rock, and is named soil type A in both the EC8 and in the draft code. The second group contains loose and cohesive soils (gravel, sand, clay). The draft code names this group soil type B; EC8 makes a more detailed classification based upon geology and shear wave velocity, and distinguishes between soil types B, C, D. They add another soil type for the case of soft soil on top of the rock and name it E in EC8 and C in the draft code. When different soil types are present in P and Q, the EC8/ICPC states the most unfavourable values of the parameters be used,

Table I. Value of the response spectra parameters for EC8/ICPC and properties of the soil types in the Draft Italian Code for bridges (N.A.: not applicable).

Parameter/ground type	*A*	*B*	*C*	*D*	*E*
		EC8/ICPC			
Description	Rock	Gravel, sand, clay	Like *B*	Like *B*	*B*, *C* or *D* on *A*
ε	1	1.25	1.25	1.35	1.25
T_C (s)	0.4	0.5	0.5	0.8	0.5
T_D (s)	2	2	2	2	2
v (m/s)	>800	360–800	180–360	<180	100–360
v_{app} (m/s)	3000	2000	2000	1500	1500
		DICB			
Description	Rock	Gravel, sand, clay	*B* on *A*	N.A.	
v (m/s)	360–800	180–360	100–180		

Table II. Value of the parameters q_i for the DICB (dot indicates that the value must be computed by symmetry).

Soil P/Q	A	B	C	A	B	C	A	B	C
Parameter		$100q_1$			$10^5 q_2$			q_3	
A	0	0.7	3.3	17	1.4	17	2.5	3.9	2.9
B	.	0	2.0	.	14.3	29	.	2.9	2.9
C	.	.	0	.	.	266	.	.	1.1

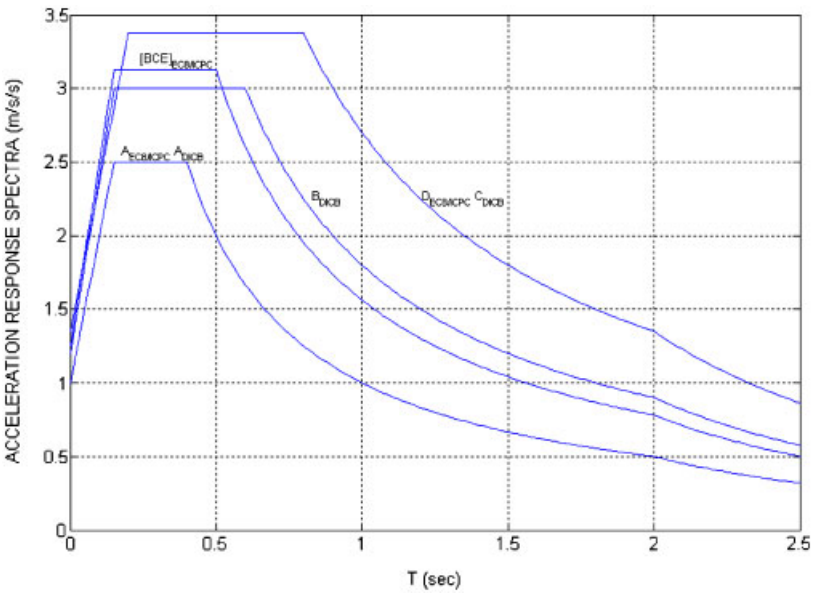

Figure 2. Acceleration response spectra given by the codes.

whereas the DICB explicitly deals with this case, via the values of the parameters q. The acceleration and displacement spectra prescribed by the codes are shown in Figures 2 and 3. The soil differential displacements are shown in Figure 4. In Figure 3 the values of T_E and T_F, the periods that define the start and the end of the decrease in the spectral displacement, are highlighted. They will be referred to in the next sections. Soils A and D of EC8/ICPC coincide, as far as response spectra are concerned, with soils A and C of the DICB; soils B, C and E of EC8/ICPC are almost coincident with soil B of the DICB. In the analyses only three ground types will be considered: A, B and D as defined in EC8/ICPC, the most different situations encountered.

For the differential displacements, the codes are much less similar. The maxima differential displacements differ by 1.25 (the factor in the last of Equations (16)), and also the trend is very different. EC8/DICB increases linearly up to the maximum, and the DICB grows in a parabolic fashion. In the range of distances where most civil engineering structures are,

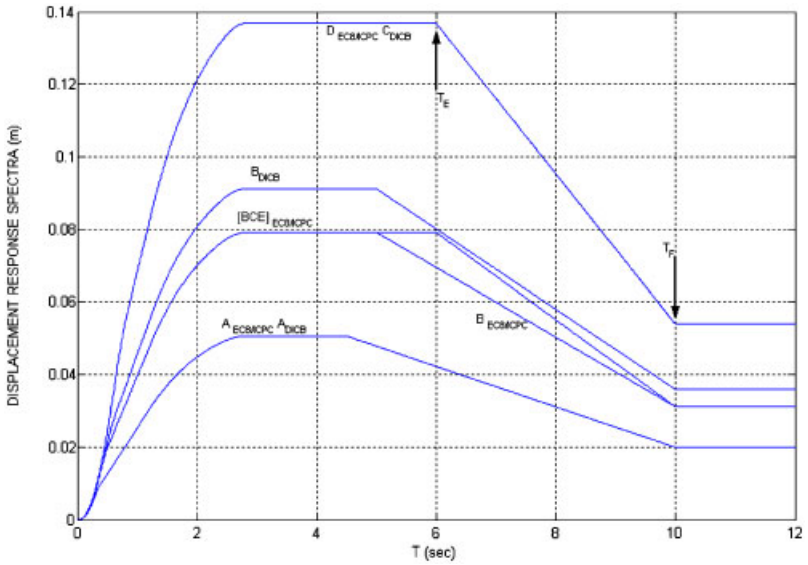

Figure 3. Displacement response spectra given by the codes.

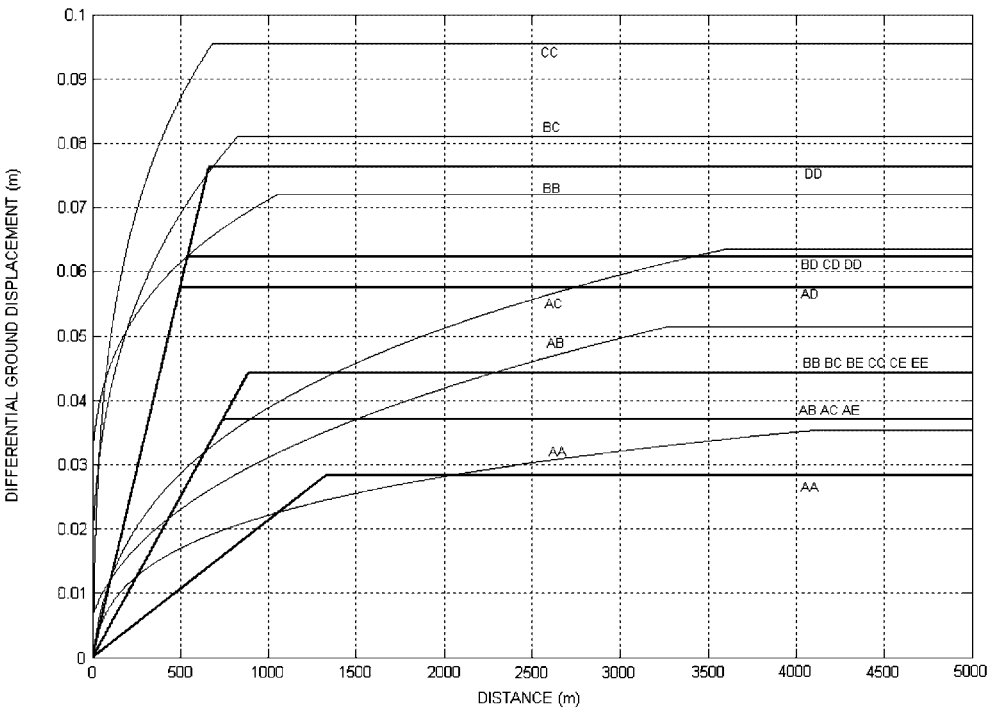

Figure 4. Soil differential displacement prescribed by the codes. Thicker lines are for EC8/ICPC.

between 5 and 100 m, from buildings columns to long bridges piers, the differences are large: at 20 m distance, EC8/ICPC gives 2 mm or less while DICB forecasts differential displacements from 2 mm to about 40 mm, depending on the soil coupling. Such large differences must be carefully investigated.

The systematic investigation of the dependence of differential displacements on the governing variables is done in the next sections: the outcome of the study is that EC8/ICPC is always unconservative, with strong underestimation in the 5–100 m range.

4. ORGANIZATION OF ANALYSES

The investigation is focussed first on the maxima differential displacements of two points P and Q on the ground and then on two points on top of sdof oscillators, points L and M, see Figure 1. The excitation is specified via its acceleration/displacement response spectra. The maxima differential displacements are expressed by Equation (15).

For the peak ground acceleration, pga, a value of $1\,\mathrm{m/s^2}$ is retained. The structural damping is taken equal to 5%. The response spectra shapes are those of EC8 [14]. Three ground types are considered, A, B and D, the most different situations encountered. These ground types essentially correspond to A, B and C of the DICB [16]. It has then been assumed that each of the points P and Q could be in each ground type.

In the model, the excitation needs to be specified in terms of power spectra. The power spectrum corresponding to each response spectrum is computed in two steps: first a numerically defined (i.e. no closed-form expression) power spectrum $G^{(\mathrm{num})}(\omega)$ corresponding to the displacement and acceleration response spectra is obtained, and then the parameters of the Kanai–Tajimi power spectrum (modified as explained later) taking $G^{(\mathrm{num})}(\omega)$ as target are computed.

$G^{(\mathrm{num})}(\omega)$ is computed with the trial and error procedure outlined in Reference [7]. The procedure converges to $G^{(\mathrm{num})}(\omega)$ adjusting, frequency by frequency, a guess power spectrum $G^{(0)}(\omega)$ on the basis of the predicted maximum displacement. For the second step, a modified version of the Kanai–Tajimi acceleration power spectrum, Equation (3), is used. The modified version reads as

$$
\begin{aligned}
G_{\text{modified-KTCP}} &= G_{\text{KTCP}}\lambda_0 \\
G_{\text{KTCP}} &= G_0 \frac{\omega_f^4 + 4\beta_f^2\omega_f^4\omega^2}{(\omega_f^2-\omega^2)^2 + 4\beta_f^2\omega_f^4\omega^2}\,\frac{\omega^4}{(\omega_g^2-\omega^2)^2 + 4\beta_g^2\omega_g^4\omega^2} \\
\lambda_0 &= 0.5 + \frac{1}{\pi}\arctan\left[\chi\,\frac{2\omega-\omega_E-\omega_F}{\omega_E-\omega_F}\right] \\
\omega_e &= \frac{2\pi}{\mathrm{T}_e};\quad \omega_f = \frac{2\pi}{\mathrm{T}_f}
\end{aligned}
\tag{19}
$$

G_{KTCP} in Equation (19) is a Gaussian white noise with constant value equal to G_0 passed through a linear filter, with circular frequency ω_f and damping β_f, representing the ground.

Clough and Penzien [21] introduced a second filter with circular frequency ω_g and damping β_g to do away with the fact that the displacement power spectrum, obtained by dividing the acceleration power spectrum by ω^4, tends to $+\infty$ with $\omega \to 0$ and that the integral of the displacement power spectrum, i.e. the variance of displacements, is infinite too.

With $\omega \to 0$ the Kanai–Tajimi–Clough–Penzien displacement power spectrum tends to a constant value whereas the displacement response spectrum corresponding to $G^{(\text{num})}(\omega)$ goes to zero, see Reference [20]; this makes it impossible to match the target displacement response spectra at high periods, above T_E of Figure 3. The correction term λ_0 solves this problem. χ is a problem-dependent parameter and the value of 10 has proved apt for the case of response spectra specified by EC8 [14].

The differential ground response (points P and Q) is computed keeping as parameters the soil types in P and Q, the value of the incoherence factor α, the surface wave velocity v_{app} (expressed as a parameter θ times the surface wave velocity specified by the EC8 code for each ground type, i.e. $v_{\text{app}} = \theta \cdot v_{\text{app\_EC8}}$) and the distance between the points. No ambiguity exists for choosing the parameters v and v_{app} in case the soils in P and Q are of the same type. For two different soil types below P (soil type 1) and Q (soil type 2), the homogenization formulas in Equations (5) and (8) are used, with a value for ξ_1 of 0.5, i.e. the soil discontinuity is at the same distance from P and from Q. The duration of the earthquake is assumed equal to 25 s and the comparisons with the codes are made by keeping the probability value at 0.5, since the spectra specified in the codes are at that probability level. The dependence of the maxima differential displacements on the probability level has also been investigated.

For the differential displacements on top of the structures, two more parameters must be considered, the modal periods of each structure. In the structural analyses, fixed values for α (equal to 0.5) and θ (equal to 1) are assumed. The variables are summed up in Tables III and IV.

Table III. Values of the variables used for the assessment of differential displacements.

#	Variable	Values assigned to variable
	Variables used to assess the differential ground displacement	
1	Soil type in P	A, B and D as defined by EC8*
2	Soil type in Q	A, B and D as defined by EC8*
3	Distance between P and Q	From 0 to 10 000 m
4	Incoherency parameter α	From 0.02 to 0.5
5	θ such that $v_{\text{app}} = \theta v_{\text{app\_EC8}}$	0.5, 1, 1.5
6	Probability levels	From 0.01 to 0.99
	Further variables used to assess the differential structural displacement (only for the case of $\alpha = 0.5$ and $\theta = 1$)	
7	Period of the first structure T_P	From 0.2 to 2
8	Period of the second structure T_Q	From 0.2 to 2

*A, B and D as defined by EC8 are equal to A, B and D of ICPC and A, B and C of DICB.

Table IV. Values of the shear and apparent wave velocities, v and v_{app}, assumed in the analysis.

Parameter/ground type	*A*	*B*	*D*
Description	Rock	Gravel, sand, clay	Gravel, sand, clay
v (m/s)	800	580	90
v_{app} (m/s)	3000	2000	1500

5. RESULTS FOR THE GROUND DIFFERENTIAL DISPLACEMENTS

For each soil coupling, the parameters governing the differential displacements of P and Q are four: the distance between P and Q, X_{PQ}, the probability level p, and two soil parameters, the incoherence factor α and the apparent surface wave velocity (expressed as $v_{app} = \theta v_{app\_EC8}$). The latter two are extremely dispersed, even within homogeneous soils, and the shear wave velocity v is a more critical variable than the surface wave velocity v_{app}; thus, α is a more important variable than θ. For these reasons the probability level is first fixed at 50%, θ at 1, and the results examined keeping only the distance between P and Q, X_{PQ}, and the incoherence factor α as variables. The results are presented as level curves of the maximum differential displacement, with X_{PQ} on the x-axis and v/α on the y-axis, in doubly logarithmic scales. The results for soil coupling DD are shown in Figure 5.

From bottom left to top centre, the level curves are first oriented at 45° (in doubly logarithmic scales) with respect to the x-axis and then they get vertical, through a transition branch. Let x, y and z the quantities on the axes, respectively, be the distance, v/α and the differential displacements. If the surface $z(x, y)$ is cut with a plane parallel to the (x,z) plane, i.e. at constant v/α, the function $z(x)$ at constant y is obtained. If this is done at $y = v/\alpha = 100$ m/s, for any ground coupling, one always is in the area with level curves at 45°. With $y = v/\alpha = 10^5$ m/s one always is in the area with vertical level curves. For this reason, the values 100 and 10^5 m/s are assumed as reference ones. The function $z(x, y = 100 \text{ m/s})$ is referred to as $z_{100}(x)$, the function $z(x, y = 10^5 \text{ m/s})$ as $z_{1e5}(x)$.

The value of z for a point of co-ordinates (x, y) can be read from Figure 5, or from the similar ones for different soils; but it can be obtained also from $z_{100}(x)$ and $z_{1e5}(x)$ depending on where the point (x, y) is. If it is in the area with level curves at 45°, e.g. point O1 in Figure 5, the differential displacement z is found projecting (x, y) at 45° (i.e. parallel to the level curves) on the line $y = v/\alpha = 100$ m/s (point O2 in Figure 5). If it is in the area with vertical level curves, e.g. point O3 in Figure 5, it must be projected parallel to the y-axis up to the line $y = v/\alpha = 10^5$ m/s (point O4 in Figure 5). The transition branch is disregarded. The value of $z(x, y)$ can therefore be computed as $z_{100} = z(x_1, y = 100 \text{ m/s})$ or as $z_{1e5} = z(x, y = 10^5 \text{ m/s})$; its correct value will be the higher between the two. Hence, the differential displacement z is equal to

$$\begin{aligned} z_{PQ}(X_{PQ}, v/\alpha) &= \max(z_{100}, z_{1e5}) \\ z_{100} &= z\left[X = \left(X_{PQ}\,\frac{100 \text{ m/s}}{v/\alpha}\right), v/\alpha = (100 \text{ m/s})\right] \\ z_{1e5} &= z[X = (X_{PQ}), v/\alpha = (10^5 \text{ m/s})] \end{aligned} \tag{20}$$

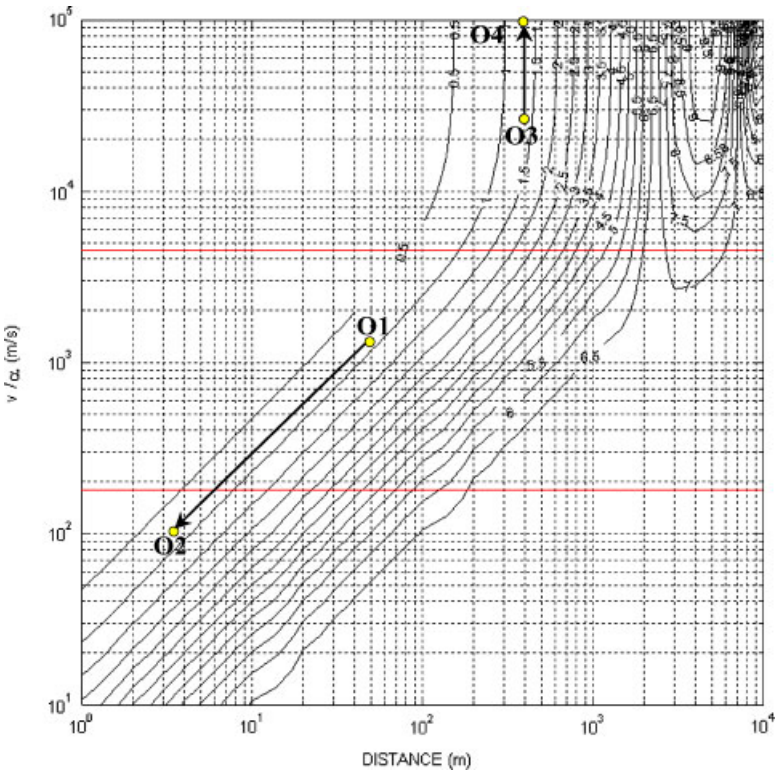

Figure 5. Level curves of differential ground displacement (10^{-2} m) for soil coupling *DD*. The two horizontal lines are drawn at $v/(\alpha = 0.02)$ and $v/(\alpha = 0.5)$, the lower and upper bounds assumed.

Equation (20) shows the influence of the incoherence factor α on the ground differential displacement, for a given distance between points X_{PQ}, and of soil shear wave velocity v. For low values of the incoherence factor α (top part of Figure 5 and third of Equations (20)), the differential displacement depends solely on the distance between points and not on α. For higher values of incoherency (bottom part of Figure 5 and second of Equations (20)) the effect of α is the same as the distance. The influence of a change in the surface wave velocity, v_{app}, is much smaller. The results obtained with the same parameters as in Figure 5, with only a change in the value of θ, show that the only difference is in the position of the upper (i.e. vertical level curves) part of the diagram, see Reference [20] for details. A decrease in θ makes the upper part move left, an increase makes it move right. The only change to Equation (20) needed to quantify its influence is the expression of z_{1e5}.

From a physical point of view, this means that an increase in the surface wave velocity, i.e. a decrease in the time lag τ_{PQ} between the accelerations in P and Q, has the effect of broadening the range of influence of α. The shear wave velocity v and the surface wave velocity v_{app} have similar effects on the differential ground displacements: all other things equal, differential ground displacements increase with decreasing v and v_{app}. Finally, the oscillatory pattern in the upper-right part of Figure 5 depends on the cosine term within σ_{PQK}

in the maximum ground differential displacement expression, Equation (14). All that has been said up to now, making reference to one soil coupling, is true for all soil couplings.

The results discussed are relative to 0.5 probability of exceedance; the level curves at different probability values p are identical to those shown for $p=0.5$ apart from a scale factor $f(p)$, which is a smooth function of p. This regularity holds for all tested soils, distances and coherency parameters. $f(p)$ is well interpolated by a third degree polynomial:

$$z_{PQ}(p)=z_{PQ}(p=0.5)f(p)$$
$$f(p)=2p^3-2.7p^2+1.38p+0.735 \tag{21}$$

Given the soil types in P and Q, the soil differential displacement can be therefore defined as a function of all the governing variables, distance, incoherence parameter α, θ and probability level, via the closed-form-approximate expressions of z_{100} and z_{1e5}. There will be one expression for z_{100} (which is independent of θ) and three expressions for z_{1e5} (at the three considered values for $\theta=0.5,1,1.5$). The approximating functions, found with a least square error procedure on its unknowns q_1,q_2,q_3, are accurate and are defined by

$$z_{PQ}(X_{PQ})\approx z_{PQ}^{(\mathrm{appr})}(X_{PQ})=\{q_1+q_2[\log(X_{PQ})]^{q_3}\leqslant z_{PQ}^{\max}\} \tag{22}$$

In Equation (22) the oscillatory pattern of z_{1e5} at large distances is disregarded. q_1 is always zero for homogeneous soils; for different soils in P and Q, it is equal to 0.007 m (AB), 0.033 m (AD), 0.02 m (BD). The highest differential displacements are given by the case with the highest incoherence factor α, 0.5, irrespective of the value of θ; these can also be computed via use of Equation (22). The differential displacements for this case are referred to as $z_{v/0.5}$.

The values of $q_2,q_3,z_{PQ}^{\max}$ for $z_{100},z_{1e5},z_{v/0.5}$, and for all soil couplings are listed in Tables V and VI. In these, the dot symbol by a matrix component indicates that it must be computed by symmetry. Equation (22) must be used with *meter* units.

The maxima differential displacements for this case are in good agreement with EC8/ICPC [14, 15]. However, with reference to soil coupling DD, from Figure 5, the maximum differential displacement occurs for the lowest value of the incoherence factor α, i.e. at $v/(\alpha=0.02)$, and is equal to 0.0725 m, slightly more than 0.069 m, the maximum for $v/(\alpha=0.5)$. The maximum differential displacement for $\theta=0.5$ and $v/(\alpha=0.02)$ (not shown here) is still a bit larger, 0.08 m, i.e an increase of 16% with respect to 0.069 m. This happens for all soil

Table V. Parameters $q_1,q_2,q_3,z_{PQ}^{\max}$ in Equation (22) to compute z_{100} and $z_{v/0.5}$.

z	z_{100}						$z_{v/0.5}$						z_{100} and $z_{v/0.5}$		
Parameter	10^5q_2			q_3			10^5q_2			q_3			$100z_{\max}$		
Soil P/Q	A	B	D	A	B	D	A	B	D	A	B	D	A	B	D
A	141.2	86.6	42	1.99	2.26	2.60	16.97	1.36	17.05	2.52	3.87	2.80	2.9	3.5	5.7
B	.	226.4	93.8	.	1.86	2.37	.	14.28	28.91	.	2.90	2.81	.	3.9	5.5
D	.	.	396.9	.	.	1.85	.	.	265.54	.	.	1.91	.	.	7.0

Table VI. Parameters $q_1, q_2, q_3, z_{PQ}^{\max}$ in Equation (22) to compute z_{1e5}. The three figures in a cell are relative to $\theta = 0.5, 1, 1.5$, respectively.

Parameter	$10^5 q_2$			q_3			$100 z_{\max}$		
Soil P/Q	*A*	*B*	*D*	*A*	*B*	*D*	*A*	*B*	*D*
A	2.5e-2	8.7e-4	9.1e-5	5.64	7.33	8.43	4.35	4.8	7.5
	3.6e-3	1.5e-4	1.9e-5	6.34	7.85	8.83	4	4.7	7.4
	9.6e-4	2.8e-5	1.6e-6	6.82	8.47	9.78	3.7	4.4	7.1
B	.	1.8e-1	3.4e-4	.	4.96	8.11	.	6	7.4
		1.4e-2	4.4e-5		5.99	8.75		5.7	7.3
		5.1e-3	1.9e-5		6.32	8.93		5.5	7.3
D	.	.	2.5e-1	.	.	5.19	.	.	10.5
			6e-2			5.65		10.4	
			1e-2			6.36			9.6

Table VII. Comparison between the maxima differential displacements (10^{-2} m) predicted by EC8/ICPC [14, 15] and those relative to ($z_{v/0.5}$ and $\theta = 1$) and ($z_{v/0.02}$ and $\theta = 0.5$).

Soil coupling	*AA*	*AB*	*AD*	*BB*	*BD*	*DD*
EC8/ICPC	2.9	3.7	5.7	4.3	6.2	7.6
$z_{v/0.5}$ and $\theta = 1$	2.9	3.4	5.6	3.9	5.5	6.9
$z_{v/0.02}$ and $\theta = 0.5$	3.4	4.3	7	5.5	7.8	8

couplings. To facilitate the comparison, the maxima differential displacements for these three cases, EC8/ICPC [14, 15], ($z_{v/0.5}$ and $\theta = 1$) and ($z_{v/0.02}$ and $\theta = 0.5$), are shown in Table VII.

The differences between the values predicted by ($z_{v/0.5}$ and $\theta = 1$) and ($z_{v/0.02}$ and $\theta = 0.5$) range from +16% (coupling *DD*) to +42% (coupling *BD*); the differences between the values predicted by (EC8/ICPC) and ($z_{v/0.02}$ and $\theta = 0.5$) range from +5% (coupling *DD*) to +25% (coupling *BD*).

For this reason, and because the maxima occur at large distances, the maximum differential displacements computed with EC8/ICPC should be increased by 25%:

$$z_{PQ}^{\mathrm{MAX}} = 1.25 \times 0.025\,\mathrm{pga}\,\sqrt{(\varepsilon_P T_{PC} T_{PD})^2 + (\varepsilon_Q T_{QC} T_{QD})^2} \tag{23}$$

The variation of the differential displacement with distance can be computed with Equation (22) and the parameters relative to $z_{v/0.5}$ in Table V, but with $z_{\max}$ computed as in Equation (23). This is what has been implemented in the DICB.

6. RESULTS FOR THE STRUCTURAL DIFFERENTIAL DISPLACEMENTS

In this section the structural differential displacements are examined. α, θ and p are kept at a fixed value, respectively, 0.5, 1 and 0.5. The problem is cast as

$$z_{LM} = (z_{PQ} + u_{LM})D \tag{24}$$

In Equation (24) D is the unknown. D makes the correct structural differential displacement, z_{LM}, equal to the differential structural displacement computed *code-style*, i.e. summing up the contribution of the ground and of the structures considered separately. The contribution of the ground is computed in the correct way, as in the previous section, and the contribution of the structures is computed with a modal analysis with CQC modal combination at fixed base. D takes into account both the correlation between structural differential displacements and between the differential displacements of soil and structures above it.

For each soil coupling, D depends on the distance and on the natural periods of the structures, $D = D(X_{PQ}, T_P, T_Q)$. The shape of $D(X_{PQ})$ has two distinct behaviours depending on the distance between periods $|T_P - T_Q|$: for values of $|T_P - T_Q|$ lower than or equal to 0.1 s, D grows with the space distance up to its asymptotic value; for values of $|T_P - T_Q|$ larger than 0.1 s, D is practically constant.

The natural periods are discretized at 0.1 s step, ranging from 0.2 to 2 s, the results divided into two groups, $|T_P - T_Q|$ lower or equal and larger than 0.1 s, and, within each group, mean and dispersion of D are computed:

$$D_m(X_{PQ}) = \frac{\max_{T_P,T_Q}[D(X_{PQ}, T_P, T_Q)] + \min_{T_P,T_Q}[D(X_{PQ}, T_P, T_Q)]}{2}$$
$$D_e(X_{PQ}) = \frac{\max_{T_P,T_Q}[D(X_{PQ}, T_P, T_Q)] - \min_{T_P,T_Q}\left[D(X_{PQ}, T_P, T_Q)\right]}{2} \tag{25}$$

For a given distance X_{PQ}, $D_m(X_{PQ})$ is halfway between the minimum and maximum of $D(X_{PQ}, T_P, T_Q)$ for any natural period; $D_e(X_{PQ})$ is the distance of the maximum and the minimum from $D_m(X_{PQ})$. The two quantities show both the trend of D and the error committed if one assumes $D(X_{PQ}, T_P, T_Q) \approx D_m(X_{PQ})$. The results are shown only for $|T_P - T_Q| \leqslant 0.1$ s in Figures 6 and 7. The results for periods such that $|T_P - T_Q| > 0.1$ s are not shown here, since their interpretation is straightforward: 1 is a reasonable upper bound for D. The correct value of D depends on the soil coupling, the distance and T_P and T_Q and ranges from about 0.6–0.98. There is a discernible pattern as a function of the distance and the soil coupling, but no regularities depending on the natural periods have been found.

For periods such that $|T_P - T_Q| \leqslant 0.1$ s the interpretation is less simple: depending on the soil coupling, the asymptotic value of D_m, from about 0.65–0.75, is reached at distances between 200 m (DD coupling) and 1000 m (AA soil coupling); before that, D_m grows with the distance. Within the first 200 m, D_e is lower than or equal to about half the corresponding value of D_m. For larger distances it decreases to about 20% the corresponding value of D_m. For this group of structures ($|T_P - T_Q| \leqslant 0.1$ s), the shape of $D_m(X_{PQ})$ is approximated with the power of log function already used. One such approximation is shown in Figure 6 for soil coupling AA. The approximations appear to work well for all the soil couplings. So, for this case, one can set

$$D(X_{PQ}) \leqslant D_m(X_{PQ}) + D_e(X_{PQ}) \leqslant 1.5 D_m(X_{PQ}) \leqslant 0.90$$
$$D_m(X_{PQ}) = q_4 + q_5 \log(X_{PQ})^{q_6} \tag{26}$$

The use of SRSS instead of CQC modal combination, would be desirable since it is simpler. The use of SRSS has proved feasible, both for the case $|T_P - T_Q| > 0.1$ s and for the case

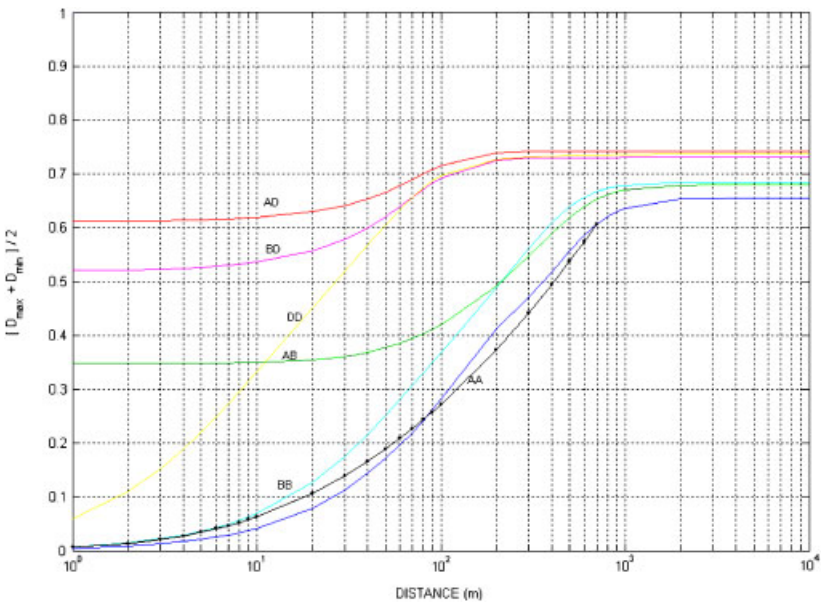

Figure 6. Value of D_m for all soil couplings and periods T_P, T_Q such that $|T_P - T_Q| \leqslant 0.1$ s.

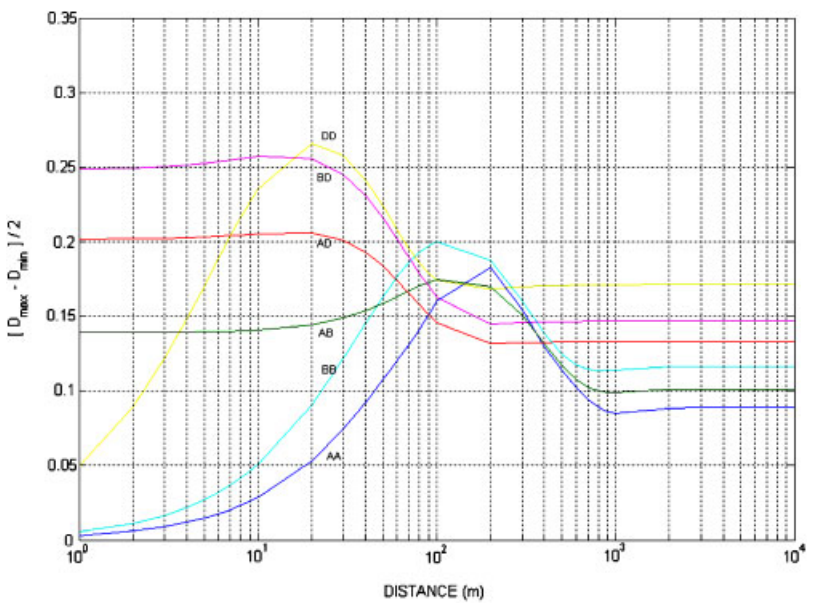

Figure 7. Value of D_e for all soil couplings and periods T_P, T_Q such that $|T_P - T_Q| \leqslant 0.1$ s.

$|T_P - T_Q| \leqslant 0.1$s. For the former case, one can assume again $D = 1$. For the case $|T_P - T_Q| \leqslant 0.1$s, Equation (26) may be used. The values of q_4, q_5, q_6, for each soil coupling and for the CQC and SRSS modal combination rules are listed in Table VIII.

Table VIII. Parameters q_4, q_5, q_6 in Equation (26) to compute D_m with T_P, T_Q such that $|T_P - T_Q| \leqslant 0.1$ s and CQC modal combination. The results relative to SRSS modal combination are between brackets.

Parameter	$q_4 100$			$q_5 10^3$			q_6		
Soil P/Q	A	B	D	A	B	D	A	B	D
A	0	34.8	61.3	7.76	0.25	1.5	2.31	3.76	2.66
		(43)	(69)	(12.6)	(0.24)		(2.16)	(3.9)	(2.70)
B	.	0	52.1	.	13.54	3.98	.	2.1	2.36
			(60)		(17.9)	(4.2)		(20)	(2.39)
D	.	.	0	.	.	70.65	.	.	1.46
						(81)			(1.47)

The case $|T_P - T_Q| \leqslant 0.1$ s is singled out from the general and simple $D = 1$ result, both because the results say so and because it is a very common situation, at least in Italy. The great majority of the Italian railway and highway bridges [32] have simply supported prestressed concrete decks, with piers that are essentially sdof systems. When the highway or railway crosses a plain the piers are typically equal structures at short distances, say 20–30 m. The use of the general $D = 1$ rule would be too unnecessarily conservative. However, use of Equation (26) requires care in verifying its assumptions.

Another important point concerns the influence of the probability level on the structural differential displacement z_{LM}. Different fractiles of the structural differential displacements may be obtained from the median value by multiplying it by the same scale factor $f(p)$ as in Equation (21), i.e.

$$z_{LM}(p) = z_{LM}(p = 0.5) f(p) \tag{27}$$

In the DICB, for the case of fragile failures, the final differential displacement is multiplied by 1.25 (see Equation (18)). Doing so, one obtains, both for the soil and the structural differential displacements, a 90% probability of them not being exceeded.

7. CONCLUSIONS

Based on well-known expressions for spatial variability of seismic motion, a theoretical model founded on basic random vibration theory, is developed. The model is used to compute the differential displacements of points on the grounds and on top of sdof linear elastic system. The study is specialized for the seismic input specified by Eurocode 8 [14], the Italian Civil Protection Code [15] and the new draft Code for bridges [16]. The case of contiguous different soils is explicitly included, since the expression of the coherency function is the same as for the case of homogeneous soil. The simple expressions of the equivalent parameter are given in Equations (5), (8)–(10).

With the exception of the Italian code for Bridges [16], drafted following the results of this study, the codes seem improvable on this aspect, both from the qualitative and quantitative viewpoint. This is surprising since the theoretical model for relative displacements is straightforward to set up and since differential displacements are the main cause of spectacular failures as the serial unseating of simply supported bridges deck.

The formulas for relative displacement between statically determined structures are then given, obtaining a unified formulation for the statistics of the relative displacements between the top of two structures, top of one structure and base of the other, base of two structures. The solution is given with the peak factor formulation: the response is the standard deviation of the process times a factor, which is a function of the probability of exceedance (see Equations (14) and (15)). A further result is that the widely adopted Kanai–Tajimi–Clough–Penzien power spectrum must be modified in order to reproduce the code displacement response spectra at large periods.

Due to regularities in the differential responses, final conclusions can be drawn and the expression of the differential response in closed form, as a function of the important variables, can be given. These results are compared with the Eurocode 8 [14], which coincides with the Italian Civil Protection Code [15], and the draft Italian code for bridges [16].

The main results are the following:

- The soil differential displacements vary smoothly to their asymptotic value, attained at distances between 600 (soil coupling DD) and 4000 m (soil coupling AA). These values are conservative and take into account the most unfavourable combinations of soil properties.
- When the soil is homogeneous, the differential displacement at zero distance is zero; when two different soil types are contiguous, the differential displacement at zero distance has a finite, non-disregardable value.
- The variation of soil differential displacement with the distance can be accurately approximated with a power of log function.
- The surface wave velocity is much less influential than the shear wave velocity and may be disregarded in design codes.
- The incoherence parameter α, within the expression v/α, is, together with the distance, the most influential variable. Its assessment for each soil type is, in the authors' opinion, at best difficult and questionable. Significant more research effort is needed on this point. To account for this problem, which is probably more due to lack of basic comprehension of physical behaviour than to intrinsic randomness, it is reasonable to keep on the safe side, as has been done in the Draft Italian Code for bridges [16].
- The maximum differential soil displacements at large distances can be obtained using the expression given by Eurocode 8 [14] increased by 25%.
- The total structural differential displacements can be computed summing the soil differential displacement and the structural differential displacement. The latter can be obtained with the SRSS rule (root of the sum of the squares of top displacements for synchronous motion) and must be corrected with a coefficient that accounts for the correlation of motions. This coefficient can be safely taken equal to 1. For structures with natural periods less distant than 0.1 s, founded on homogeneous soils, the correction coefficient can be reduced.
- The above is said with reference to the median value of the differential displacements of both the soil and the structures. To compute them with varying probability of exceedance, one may multiply the median value by the probability factor $f(p)$. The $f(p)$ has a simple polynomial expression independent of the soil type and the structural periods. If the median value is multiplied by 1.25, the differential displacements with 10% probability of exceedance is obtained.

- For differential displacement for bridges, Eurocode 8 [14] and the Italian Civil Protection Code [15] appear inaccurate and unconservative. This is especially true in the range of distances where most civil engineering structures are below 100 m. For instance, with a pier distance of 32 m, in soft soil, and peak ground acceleration equal to $0.4g$, the estimation of soil differential displacements is 14 mm for Eurocode 8 and the Italian Civil Protection Code; the model prediction is instead 112 mm, consistent with the draft Italian Code for bridges [16].

As a final remark, it is highlighted that earthquake spatial variability does appear to be a significant problem for failure modes governed by differential displacements, and also for structures of minor importance like small bridges. Since its inclusion in the design phase brings about small or no extra cost for most situations, it is worth to stress the importance of a rapid code update on this subject.

REFERENCES

1. Abrahamson NA, Schneider JF, Stepp JC. Empirical spatial coherency functions for application to soil-structure interaction analyses. *Earthquake Spectra* 1991; **7**(1):1–27.
2. Oliveira CS, Hao H, Penzien J. Ground motion modeling for multiple-input structural analysis. *Structural Safety* 1991; **10**(1–3):79–93.
3. Luco JE, Wong HL. Response of a rigid foundation to a spatially random ground motion. *Earthquake Engineering and Structural Dynamics* 1986; **14**(6):891–908.
4. Santa-Cruz S, Heredia-Zavoni E, Harichandran RS. Low-frequency behavior of coherency for strong ground motions in Mexico City and Japan. *12th World Conference on Earthquake Engineering*, New Zealand Society for Earthquake Engineering, Upper Hutt, New Zealand, 2000 (Paper No. 0076).
5. Vanmarcke EH, Fenton GA. Conditioned simulation of local fields of earthquake ground motion. *Structural Safety* 1991; **10**(1–3):247–264.
6. Der Kiureghian A, Neuenhofer A. Response spectrum method for multi-support seismic excitations. *Earthquake Engineering and Structural Dynamics* 1992; **21**(8):713–740.
7. Der Kiureghian A, Neuenhofer A. A response spectrum method for multiple-support seismic excitations. *UCB/EERC-91/08*, Berkeley, Earthquake Engineering Research Center, University of California, August 1991, 66pp.
8. Monti G, Nuti C, Pinto PE, Vanzi I. Effects of non synchronous seismic input on the inelastic response of bridges. *II International Workshop on Seismic Design of Bridges*, Queenstown, New Zealand, 1994.
9. Monti G, Nuti C, Pinto PE. Nonlinear response of bridges under multisupport excitation. *Journal of Structural Engineering* 1996; **122**(10):1147–1159.
10. Hao H. A parametric study of the required seating length for bridge decks during earthquake. *Earthquake Engineering and Structural Dynamics* 1998; **27**(1):91–103.
11. Harichandran RS, Hawwari A, Sweidan BN. Response of long-span bridges to spatially varying ground motion. *Journal of Structural Engineering* 1996; **122**(5):476–484.
12. Sextos AG, Pitilakis KD, Kappos AJ. Inelastic dynamic analysis of RC bridges accounting for spatial variability of ground motion, site effects and soil-structure interaction phenomena. Part 1: Methodology and analytical tools. Part 2: Parametric study. *Earthquake Engineering and Structural Dynamics* 2003; **32**(4):607–652.
13. Housner G *et al.* Competing against time. In *Report to Governor G. Deukmejian from the Governor's Board of Inquiry on the 1989 Loma Prieta Earthquake*, Thiel Jr CC (ed.). Department of General Services, State of California: North Highlands, CA, 1990.
14. Comité Européen de Normalisation, CEN. *Eurocode 8*: *Design of Structures for Earthquake Resistance*, Draft n. 2, doc cen/tc250/sc8/n320, May 2002.
15. Presidenza del Consiglio dei Ministri. *Primi elementi in materia di criteri generali per la classificazione sismica del territorio nazionale e di normative tecniche per le costruzioni in zona sismica*. Ordinanza, March 2003 (in Italian).
16. Consiglio Superiore dei Lavori Pubblici. *Aggiornamento delle Norme Tecniche per le Costruzioni in zone sismiche*. Draft version of October 2003, available at http://host.uniroma3.it/master/mica/mica.asp > normativa and at http://www.infrastrutturetrasporti.it/main/facciamo/consup/consup.html > normativa (in Italian).
17. Kanai K. Semi-empirical formula for the seismic characteristics of the ground. *University of Tokio Bulletin of Earthquake Research Institute* 1957; **35**:309–325.

18. Tajimi H. A statistical method of determining the maximum response of a building structure during an earthquake. *Proceedings of the Second World Conference on Earthquake Engineering*, Tokyo, vol. II, 1960; 781–797.
19. Ang AHS, Tang WH. *Probability Concepts in Engineering Planning and Design*, vol. 1. Wiley: New York, 1975.
20. Nuti C, Vanzi I. Influence of earthquake spatial variability on the differential displacements of soil and single degree of freedom structures. *Rapporto del Dipartimento di Strutture*, DIS 1/2004, Università di Roma Tre, Rome, Italy, 2004.
21. Clough RW, Penzien J. *Dynamics of Structures*. McGraw-Hill: New York, 1975; 634pp.
22. Uscinski BJ. *The Elements of Wave Propagation in Random Media*. McGraw-Hill: New York, 1977.
23. Zerva A. Effect of spatial variability and propagation of seismic ground motions on the response of multiply supported structures. *Probabilistic Engineering Mechanics* 1991; **6**(3–4):212–221.
24. Zerva A. Seismic ground motion simulations from a class of spatial variability models. *Earthquake Engineering and Structural Dynamics* 1992; **21**(4):351–361.
25. Zerva A. Response of multi-span beams to spatially incoherent seismic ground motions. *Earthquake Engineering and Structural Dynamics* 1990; **19**(6):819–832.
26. Zerva A. Development of differential response spectra from spacial variability models. *Proceedings of the Tenth World Conference on Earthquake Engineering*, vol. 9. A.A. Balkema: Rotterdam, 1992; 5469–5474.
27. Luco JE, Mita A. Response of circular foundation to spatially random ground motion. *Journal of Engineering Mechanics* 1987; **113**(1):1–15.
28. Lupoi A, Franchin P, Monti G, Pinto PE. Relevance of spatial variability of ground motion on seismic design of bridges. *Concrete Structures in Seismic Regions*: *FIB 2003 Symposium*, Athens, Greece, 2003; 12pp.
29. Crandall SH, Mark WD. *Random Vibration in Mechanical Systems*. Academic Press: New York, 1963; 166pp.
30. Vanmarcke EH, Fenton GA, Heredia-Zavoni E. SIMQKE-II, conditioned earthquake ground motion simulator: user's manual, version 2.1. Princeton University: Princeton, NJ, 1999; 25pp.
31. Wilson EL, Der Kiureghian A, Bayo E. A replacement for the SRSS method in seismic analysis. *Earthquake Engineering and Structural Dynamics* 1981; **9**:187–192.
32. Donferri M, Giannini R, Nuti C, Pinto PE. Analysis of seismic risk on the bridges of Autostrade network. *Autostrade*. Società Autostrade: Rome, Italy, 1998; **2**:7–15.

